

Correlations between neutrons and protons near Fermi surface and Q_α of super-heavy nuclei

Ning Wang,^{1,2,*} Min Liu,¹ Xizhen Wu,³ and Jie Meng⁴

¹*Department of Physics, Guangxi Normal University, Guilin 541004, P. R. China*

²*State Key Laboratory of Theoretical Physics,
Institute of Theoretical Physics, Chinese Academy of Sciences,
Beijing 100190, People's Republic of China*

³*China Institute of Atomic Energy, Beijing 102413, P. R. China*

⁴*State Key Laboratory of Nuclear Physics and Technology,
School of Physics, Peking University, Beijing 100871, China*

Abstract

The shell corrections and shell gaps in nuclei are systematically studied with the latest Weizsäcker-Skyrme (WS4) mass model. We find that most of asymmetric nuclei with (sub)-shell closures locate along the shell stability line (SSL), $N = 1.37Z + 13.5$, which might be due to a strong correlation between neutrons and protons near Fermi surface. The double magicity of nuclei ^{46}Si and ^{78}Ni is predicted according to the corresponding shell gaps, shell corrections and nuclear deformations. The unmeasured super-heavy nuclei $^{296}118$ and $^{298}120$, with relatively large shell gaps and shell corrections, also locate along the SSL, whereas the traditional magic nucleus ^{298}Fl evidently deviates from the line. The α -decay energies of super-heavy nuclei with $Z = 113 - 126$ are simultaneously investigated by using the WS4 model together with the radial basis function corrections. For super-heavy nuclei with large shell corrections, the smallest α -decay energy for elements $Z = 116, 117$ and 118 in their isotope chains locates at $N = 178$ rather than 184.

*wangning@gxnu.edu.cn

I. INTRODUCTION

For nuclear physics, one of the most important tasks is to explore the nuclear landscape. Up to now, the masses of 2438 nuclei have already been measured according to the latest nuclear mass database AME2012 [1], and about 4000 \sim 5000 masses are still unknown. The masses of these unmeasured nuclei play a key role for the study of super-heavy nuclei (SHN) [2–4], the r-process in nuclear astrophysics [5–7] and nuclear symmetry energy [8–10]. For the synthesis of SHN, the first question that should be answered is where the central position of the island of stability locates. Traditionally, the island of stability for SHN is predicted to be around neutron number $N = 184$ and proton number $Z = 114$ [11], 120 or 126 [12–14], according to the large shell corrections (in absolute value) and/or the large shell gaps in super-heavy nuclei, since the survival of these nuclei is directly due to the shell effects. From the predicted evaporation residue cross-sections, Adamian et al. concluded that $Z = 114$ is not a proper magic number and the next magic nucleus beyond ^{208}Pb is the nucleus with $Z \geq 120$ [15]. The uncertainty of model parameters and the decreasing trend of the shell gaps with increasing of nuclear size cause some difficulties in the determination of the central position of the island. The improvement of model predictive power and the investigation of the physics behind model parameters are helpful for the determination of the island and of the new magic numbers in extremely neutron-rich nuclei.

In addition to the properties of nuclear force represented by the model parameters, the concept of symmetry in physics is a very powerful tool for understanding the behavior of Nature. The isospin symmetry discovered by Heisenberg plays an important role in nuclear physics. In the absence of Coulomb interactions between the protons, a perfectly charge-symmetric and charge-independent nuclear force would result in the binding energies of mirror nuclei being identical [16, 17]. For neutron-rich nuclei around the doubly-magic nuclei, the correlation between valence-nucleons and the corresponding doubly-magic core, and as well as the correlation/symmetry between active-protons and active-neutrons near Fermi surface should also affect the nuclear masses. It is therefore necessary to investigate these correlations.

For the synthesis of SHN, the α -decay chain is a key quantity to identify the produced SHN. The masses of SHN directly influence the evaluation of the corresponding α -decay energy Q_α . Inspired by the Skyrme energy-density functional, a macroscopic-microscopic

mass model, Weizsäcker-Skyrme (WS) model [18–21] was proposed. In this model, the isospin dependence of model parameters and the mirror corrections from the isospin symmetry in nuclear physics play a crucial role for improving the accuracy of mass predictions for neutron-rich nuclei and super-heavy nuclei. By adopting the latest version (WS4) of the model [21] together with the radial basis function corrections [22, 23] which is a prominent global interpolation and extrapolation scheme to effectively describe the systematic error of a global mass model, the 2353 measured masses ($N \geq 8$ and $Z \geq 8$) in 2012 Atomic Mass Evaluation (AME) can be reproduced with an rms deviation of 170 keV. With an accuracy smaller than 300 keV for the Q_α of SHN, the WS4^{RBF} model is one of the most reliable mass models for the study of SHN [24–26]. It is therefore interesting to systematically investigate the surface of Q_α in super-heavy region with this model.

In this work, we first study the shell corrections and shell gaps in unmeasured neutron-rich nuclei and super-heavy nuclei by using the WS4^{RBF} model. Simultaneously, the relationship among known doubly-magic nuclei such as ^{132}Sn , ^{208}Pb and ^{270}Hs [2, 3] will be analyzed from the point of view of the correlations between nucleons near Fermi surface. Then, the Q_α of super-heavy nuclei around the possible central position of the island of stability will be predicted.

II. SHELL CORRECTIONS AND SHELL GAPS IN NUCLEI

In the Weizsäcker-Skyrme mass model, the shell correction is obtained with the traditional Strutinsky’s procedure in which the single-particle levels are calculated from an axially deformed Woods-Saxon potential [27]. In Fig. 1, we show the contour plot of the calculated shell corrections from the WS4 model for nuclei over the whole nuclear landscape. Obviously, the shell corrections (in absolute value) for the known doubly-magic nuclei such as ^{132}Sn , ^{208}Pb and ^{270}Hs are larger than those of their neighboring nuclei. In addition to these known doubly-magic nuclei, the shell corrections for ^{46}Si and ^{78}Ni are also evidently large. ^{78}Ni could be doubly-magic nucleus since both the proton number $Z = 28$ and neutron number $N = 50$ are magic numbers in known mass region. Very recently, the experimental investigation on the single-neutron states in ^{79}Zn at CERN supports the picture of a robust $N = 50$ shell closure for ^{78}Ni [30]. For ^{46}Si , the neutron number $N = 32$ could be new magic number, since both the measured large shell gap in ^{52}Ca [28] and the calculations from the WS* model [29] indicate $N = 32$ being a magic number in neutron-rich nuclei.

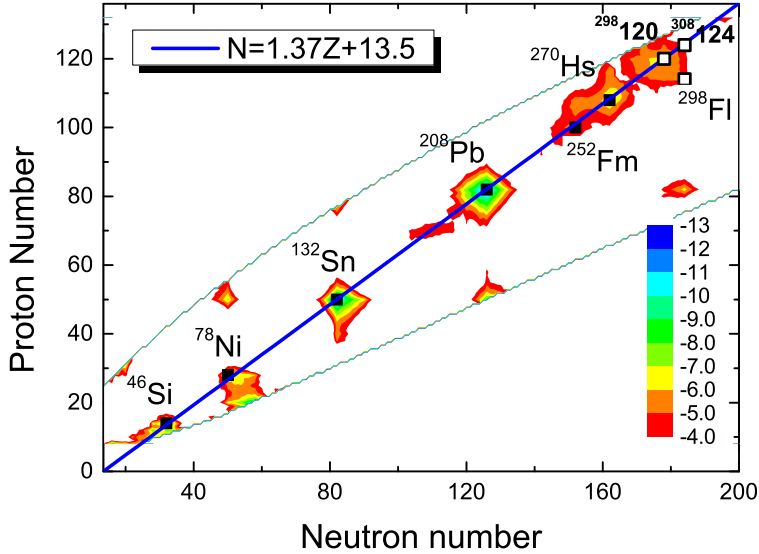


FIG. 1: (Color online) Shell corrections of nuclei from the WS4 calculations. The solid and open squares denote the positions of nuclei with (sub)-shell closure according to the predicted shell gaps.

Some investigations suggested that $Z = 14$ could also be proton magic number [31–33]. The neutron separation energy of Silicon and Nickel isotopes are also calculated with the WS4^{RBF} model, and the results are presented in Fig. 2. The squares and circles denote the measured neutron (S_n) and two-neutron (S_{2n}) separation energies, respectively, which can be remarkably well reproduced by the model predictions (the curves). According to the predicted neutron separation energy, ^{46}Si could be the neutron drip-line nucleus and ^{78}Ni is a well bound nucleus comparing with ^{46}Si . The shell gaps in ^{46}Si and ^{78}Ni will be discussed later.

More interestingly, one can see from Fig. 1 that the asymmetric nuclei with large shell corrections locate along the straight line $N = 1.37Z + 13.5$, with an uncertainty of neutron number $\Delta N < 2$. To explore the physics behind this line, we study the correlation between neutrons and protons near the Fermi surface in these doubly-magic nuclei. It is known that nucleons near the Fermi surface can significantly influence the properties of nuclei, whereas the influence from an individual nucleon located at the deep part of potential well might be negligible. In this work, the nucleons in the same major shell which is nearest to the Fermi surface is defined as active nucleons, and the rest of nucleons form a relatively

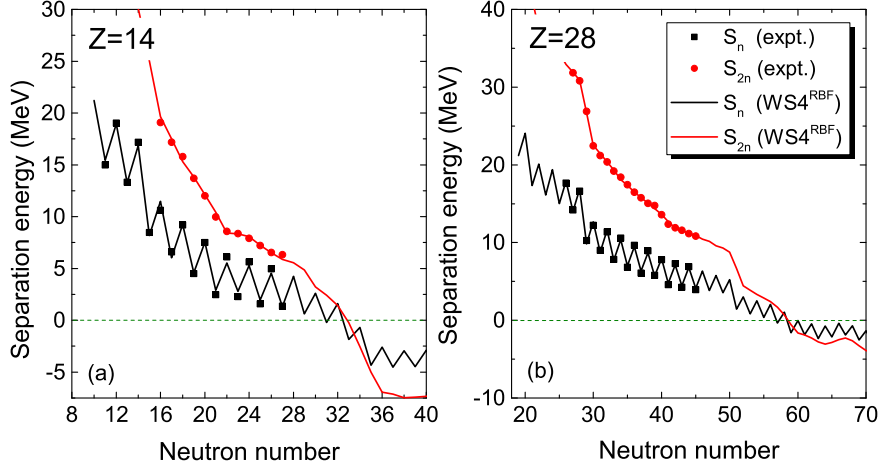


FIG. 2: (Color online) Neutron separation energy of Silicon and Nickel isotopes. The squares and circles denote the measured neutron (S_n) and two-neutron (S_{2n}) separation energies, respectively. The curves denote the predictions of the WS4^{RBF} model.

inactive core. As an example, the structure of ^{208}Pb could be described as the core with $N = 82$ and $Z = 50$ together with the active-nucleons near the Fermi surface. The ratio of active-neutrons to active-protons is $N_a/Z_a = (126 - 82)/(82 - 50) = 1.375$, and the isospin asymmetry of the core $I_{\text{core}} = (82 - 50)/132 = 0.242$. Here, we introduce an effective ratio $T_{\text{eff}} = N_a/Z_a - I_{\text{core}}$. We find that one gets almost the same value $T_{\text{eff}} = 1.17 \pm 0.06$ for all these doubly-magic nuclei. For symmetric nuclei, one gets $T_{\text{eff}} = 1$ due to the isospin symmetry. For heavy nuclei with $N > Z$, more neutrons are required to balance the strong Coulomb repulsion and the effective ratio T_{eff} should be larger than one. The similar value of T_{eff} indicates that there exists a strong correlation between the neutrons and protons near the Fermi surface. This correlation could be due to the competition between the isospin symmetry and Coulomb interaction in the active-nucleon space. The line $N = 1.37Z + 13.5$ which is called shell stability line (SSL) and the similar T_{eff} value imply that the symmetry in active-nucleon space could also influence the binding energies of asymmetric nuclei.

To understand the magic numbers in extremely neutron-rich region and super-heavy region, we simultaneously investigate the shell gaps in nuclei. In macroscopic-microscopic

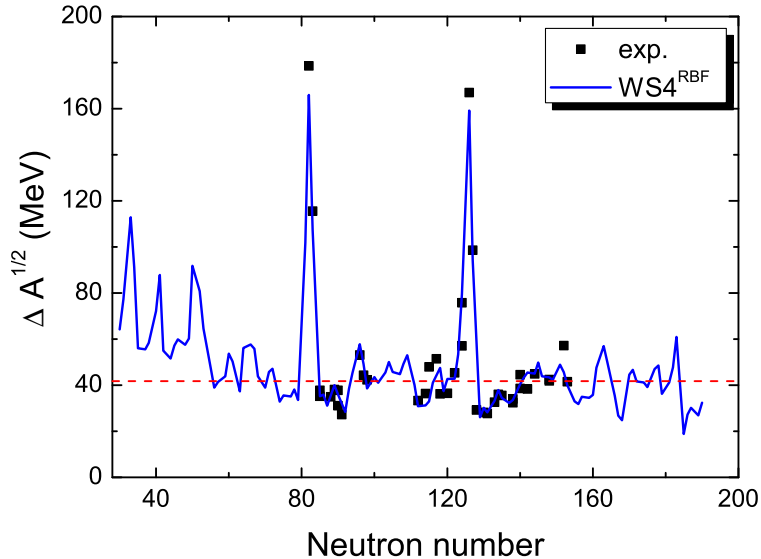


FIG. 3: (Color online) Scaled shell gaps of nuclei along the shell stability line. The squares and solid curve denote the experimental data and $WS4^{RBF}$ predictions, respectively. The dashed line denotes the mean value of measured shell gaps for all known nuclei.

models, the shell correction provides a natural measure for magicity. A more direct measure of a shell closure is the observation of a sudden jump in the two-nucleon separation energies [34]. The empirical shell gaps in nuclei are defined as the sum of the neutron and proton shell gaps based on the difference of the binding energies (in negative values) of nuclei,

$$\Delta(N, Z) = \Delta_n(N, Z) + \Delta_p(N, Z), \quad (1)$$

with

$$\Delta_n(N, Z) = B(N + 2, Z) + B(N - 2, Z) - 2B(N, Z) \quad (2)$$

and

$$\Delta_p(N, Z) = B(N, Z + 2) + B(N, Z - 2) - 2B(N, Z). \quad (3)$$

Usually, the two-nucleon gaps show a pronounced peak for magic numbers and can be considered as indicators of a shell closure [34]. Here, we would like to emphasize that the large shell gaps in light nuclei with $N = Z$ is partly due to the Wigner effects which was

TABLE I: Nuclei with relatively large shell gaps around the shell stability line. Δ_{scale} denotes the scaled shell gap (in MeV) from the WS4^{RBF} predictions. ΔE and β_2 denotes the corresponding shell correction (in MeV) and the quadrupole deformation of nucleus according to the WS4 model, respectively.

Nuclide	Δ_{scale}	ΔE	β_2
⁴⁶ Si	105.1	-7.96	-0.01
⁶⁰ Ca	97.9	-1.32	-0.01
⁷⁸ Ni	115.1	-7.98	0.01
¹³² Sn	166.0	-12.10	0.01
²⁰⁸ Pb	159.2	-12.43	0.00
²⁵² Fm	55.3	-5.30	0.24
²⁷⁰ Hs	61.1	-6.95	0.22
²⁹⁶ 118	48.0	-5.93	-0.08
²⁹⁸ 120	48.6	-5.89	-0.08
³⁰⁸ 124	67.0	-4.31	0.00

evidently observed in [35]. In this work, we focus on the shell gaps in nuclei with $N > Z$. At the same time, we introduce a scaled shell gap $\Delta_{\text{scale}}(N, Z) = \Delta(N, Z)A^{1/2}$ in order to study the change of $\Delta(N, Z)$ with the similar scale for both light and heavy nuclei [35]. The mean value of measured shell gaps for known nuclei is $\langle \Delta_{\text{scale}} \rangle = 41.9$ MeV. The corresponding value for 39 known nuclei around the SSL is $\langle \Delta_{\text{scale}}^{\text{SSL}} \rangle = 50.4$ MeV, which is obviously larger than the mean value for all known nuclei. The predicted mean value for the 118 nuclei along the SSL is $\langle \Delta_{\text{scale}}^{\text{SSL}} \rangle(\text{WS4}^{\text{RBF}}) = 49.1$ MeV. The calculated scaled shell gaps in nuclei around the SSL are also shown in Fig. 3 as a function of neutron number. The measured shell gaps can be remarkably well reproduced by the WS4^{RBF} calculations. The dashed line denotes the mean value for all known nuclei. The peaks that evidently larger than the mean value $\langle \Delta_{\text{scale}} \rangle$ might imply the appearance of (sub)-shell closures in the corresponding nuclei. In Table I, we list some nuclei with relatively large shell gaps around the SSL from the WS4^{RBF} predictions. The corresponding shell corrections ΔE and quadrupole deformations β_2 from the WS4 calculations are also presented. From the table one sees that both the predicted shell gaps and shell corrections (in absolute value) are very large for ⁴⁶Si and ⁷⁸Ni.

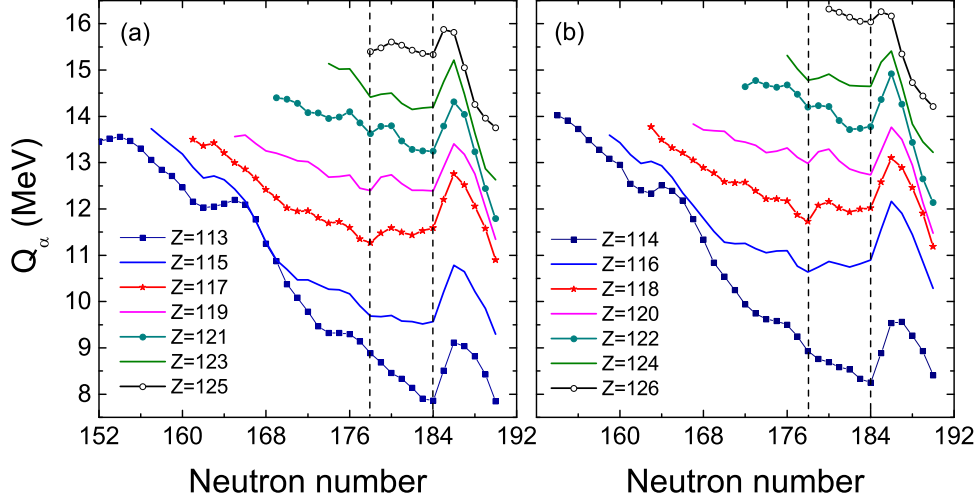


FIG. 4: (Color online) α -decay energies of odd- Z super-heavy nuclei (a) and those of even- Z nuclei (b) from the WS4^{RBF} predictions.

Simultaneously, these two nuclei are generally spherical in shape according to the predicted ground state deformations. These calculations indicate that ^{46}Si and ^{78}Ni are doubly-magic nuclei. For SHN around the SSL, both the shell corrections (in absolute value) and shell gaps in $^{296}118$ and $^{298}120$ are relatively large.

III. α -DECAY ENERGIES OF SUPER-HEAVY NUCLEI

In this work, the α -decay energies Q_α SHN are systematically investigated with the WS4^{RBF} model. Previously, Oganessian and Utyonkov investigated the discrepancy between theory and experiment in α -decay energies $\Delta Q_\alpha = Q_\alpha^{\text{exp}} - Q_\alpha^{\text{th}}$ for all of the nuclei produced as evaporation residues in the ^{48}Ca -induced reactions and their daughter products. It is found that for all of the nuclei, including odd- N and/or odd- Z ones, the discrepancies ΔQ_α are within +0.5 to -0.4 MeV from the WS4^{RBF} calculations [3]. In Table II and Table III, we list the α -decay chains for some SHN with even- Z . The corresponding shell corrections and deformation energies E_{def} (the difference in energy of a nucleus between its spherical and equilibrium shapes [2]) are also presented. The predicted α -decay energies based on the ground state energies of nuclei from four macroscopic-microscopic models are also listed

for comparison. From the tables, one sees that for the considered SHN with $Z \leq 118$, the predicted Q_α from the four different macroscopic-microscopic models are close to each other. For element 120, the results of the microscopic-macroscopic calculations based on the two-center shell model (TCSM) are evidently smaller than those of the other three models.

The predicted Q_α of SHN from the WS4^{RBF} calculations are simultaneously shown in Fig. 4. The dashed lines denote the positions of $N = 178$ and 184 . For nuclei with $Z \leq 115$ and $N < 186$, the smallest Q_α locates at $N = 184$. Whereas, for SHN with $116 \leq Z \leq 118$ and $N < 186$, the smallest Q_α also locates at $N = 178$. For SHN with $Z = 120$, there are two minima for the α -decay energy: $Q_\alpha = 12.98$ MeV at $N = 178$ which is along the SSL (see Fig. 1) and $Q_\alpha = 12.74$ MeV at $N = 184$. For the already synthesized SHN $^{294}118$ through hot fusion reaction $^{48}\text{Ca} + ^{249}\text{Cf}$ [36], the neutron number $N = 176$ is very close to the position of $N = 178$. It is therefore very interesting and important to produce more neutron-rich SHN such as $^{296}118$ and $^{297}118$ to check the trend of Q_α with neutron number, since the predicted smallest α -decay energy $Q_\alpha = 11.73$ MeV for element $Z = 118$ locates at $N = 178$. The predicted quadrupole deformation $\beta_2 = -0.08$ (see Table I) indicates that $^{296}118$ is not exactly spherical at its ground state. The deformation energy of 0.76 MeV indicates that $^{296}118$ is more stable with a slightly oblate shape in the fission path, since an extra-energy is required from oblate shape to the saddle point (with prolate shapes) and the fission path is longer comparing with the case from spherical shape. In addition, one can see from Fig. 4 that the smallest Q_α for element $Z \geq 120$ locates at $N = 184$ again. Interestingly, we find that the nucleus $^{308}124$ locates along the SSL and the corresponding shell gap is also large. These investigations indicate that the corrections between active-neutrons and active-protons influence not only the shell gaps but also the α -decay energies of SHN.

We also note that the traditional spherical magic nucleus ^{298}Fl ($Z = 114$ and $N = 184$) deviates evidently from the SSL (see Fig. 1). Although the shell gap $\Delta_{\text{scale}} = 96.2$ MeV in ^{298}Fl is larger than that in ^{270}Hs and $^{298}120$, the absolute value of its shell correction (5.16 MeV) is obviously smaller than those of ^{270}Hs and $^{298}120$. The inconsistency between shell gaps and shell corrections in SHN seems to imply that the deformation effect can not be neglected in the determination of magic numbers in super-heavy region. To investigate the next magic numbers beyond $Z = 82$, both the shell corrections and shell gaps, and as well as the deformations should be considered, simultaneously.

TABLE II: Shell corrections ΔE , deformation energies E_{def} from the WS4 calculations and α -decay energies Q_α of some even-even SHN (in MeV). Q_α^{WS} denotes the predicted Q_α from the WS4^{RBF} model. Q_α^{MM} denotes the Q_α of the macroscopic-microscopic calculations in Refs. [37, 38]. Q_α^{TCSM} and Q_α^{FRDM} denotes the results of two-center shell model (TCSM) [39] and of the finite range droplet (FRDM) model [40], respectively. The experimental Q_α^{exp} are also presented.

A	Z	ΔE	E_{def}	Q_α^{WS}	Q_α^{MM}	Q_α^{TCSM}	Q_α^{FRDM}	Q_α^{exp}
308	126	-3.41	0.07	16.14	—	13.33	—	—
304	124	-4.79	0.07	14.91	—	13.50	13.64	—
300	122	-5.36	0.30	14.20	—	13.62	13.99	—
296	120	-6.23	1.02	13.32	13.23	11.78	13.69	—
292	118	-6.02	1.74	12.21	12.15	12.03	12.37	—
288	116	-5.27	1.36	11.26	11.54	10.92	11.32	—
284	114	-4.51	0.47	10.54	11.53	10.71	9.44	—
310	126	-3.23	0.00	16.04	—	13.09	—	—
306	124	-4.64	0.15	14.67	—	12.84	16.33	—
302	122	-5.08	0.25	14.21	—	12.76	14.05	—
298	120	-5.89	0.45	12.98	13.44	11.33	13.36	—
294	118	-5.75	1.24	12.17	12.11	11.53	12.28	11.81(6) [41]
290	116	-5.53	1.39	11.06	11.08	10.90	11.12	11.00(8) [41]
286	114	-4.72	0.67	9.94	10.86	10.38	9.40	10.35(6) [41]
312	126	-2.66	1.24	16.16	—	14.36	16.53	—
308	124	-4.31	0.00	14.64	—	12.37	16.14	—
304	122	-5.05	0.33	13.71	—	11.98	14.82	—
300	120	-5.27	0.18	13.29	13.11	11.09	13.40	—
296	118	-5.93	0.76	11.73	12.06	11.01	12.29	—
292	116	-5.33	0.87	11.10	11.06	10.77	10.83	10.80(7) [41]
288	114	-5.04	0.78	9.62	10.32	10.33	9.17	10.09(7) [41]

TABLE III: The same as Table II, but for Odd-A nuclei.

A	Z	ΔE	E_{def}	Q_{α}^{WS}	Q_{α}^{MM}	Q_{α}^{TCSM}	Q_{α}^{FRDM}	Q_{α}^{exp}
309	126	-3.26	0.02	16.05	—	13.21	—	—
305	124	-4.70	0.14	14.77	—	13.00	13.44	—
301	122	-5.14	0.23	14.23	—	13.21	13.90	—
297	120	-5.79	0.71	13.12	13.49	11.53	13.54	—
293	118	-6.01	1.52	12.21	11.93	11.69	12.28	—
289	116	-5.35	1.41	11.15	11.22	10.85	11.27	—
285	114	-4.57	0.58	10.25	11.11	10.52	9.35	10.56(5) [42]
311	126	-2.87	0.42	16.26	—	13.84	17.08	—
307	124	-4.33	0.03	14.66	—	12.54	16.06	—
303	122	-5.05	0.33	13.91	—	12.22	14.71	—
299	120	-5.48	0.24	13.23	13.23	11.23	13.11	—
295	118	-5.85	1.01	11.88	12.22	11.25	12.19	—
291	116	-5.37	1.16	11.09	10.91	10.75	11.12	10.89(7) [41]
287	114	-4.83	0.76	9.74	10.56	10.31	9.31	10.16(6) [41]
313	126	-2.42	2.03	15.34	—	14.45	15.97	—
309	124	-3.18	0.06	15.17	—	13.16	16.49	—
305	122	-4.59	0.12	13.74	—	11.35	14.94	—
301	120	-5.14	0.21	13.04	13.11	10.98	13.67	—
297	118	-5.58	0.57	12.08	11.91	10.88	12.11	—
293	116	-5.61	0.77	10.77	10.09	10.51	10.94	10.67(6) [41]
289	114	-5.01	0.64	9.58	10.04	10.11	8.87	9.96(6) [41]

IV. SUMMARY

In summary, we investigated the shell corrections, shell gaps and deformations of nuclei systematically with the latest Weizsäcker-Skyrme (WS4) mass model. We find that the correlation between active-neutrons and active-protons near Fermi surface might cause many

nuclei ($N > Z$) with (sub)-shell closures locating along the shell stability line $N = 1.37Z + 13.5$. Along this line, the double magicity of nuclei ^{46}Si with new magic number $N = 32$ and of ^{78}Ni are predicted, according to the corresponding shell gaps, shell corrections and nuclear deformations. For super-heavy region, the correlation influences both the shell gaps and the α -decay energies of SHN. For the considered SHN with $116 \leq Z \leq 118$, the corresponding Q_α has the smallest value at $N = 178$ rather than 184. More neutron-rich SHN such as $^{296}118$ and $^{297}118$ could be crucial and urgently required to check the reliability of the model predictions. The calculated deformation energies suggest that the slightly oblate shapes for $^{296}118$ and $^{298}120$ at their ground state provide a more stable configuration than spherical shape in the fission path.

ACKNOWLEDGEMENTS

This work was supported by National Natural Science Foundation of China (Nos. 11275052, 11365005, 11422548, 11335002, 11265004) and National Key Basic Research Program of China (Grant No. 2013CB834400). N. W. thanks Zhu-Xia Li, Shan-Gui Zhou, Nikolai Antonenko and Gurgen Adamian for helpful discussions and acknowledges the support of the Open Project Program of State Key Laboratory of Theoretical Physics, Institute of Theoretical Physics, Chinese Academy of Sciences, China (No. Y4KF041CJ1). The nuclear mass tables with the WS formulas are available from <http://www.imqmd.com/mass/>.

-
- [1] G. Audi, M. Wang, A. H. Wapstra, F. G. Kondev, M. Mac-Cormick, X. Xu, and B. Pfeiffer, *Chin. Phys. C* **36**, 1287 (2012).
 - [2] A. Sobiczewski, K. Pomorski, *Prog. Part. Nucl. Phys.* **58**, 292 (2007).
 - [3] Yu. Ts. Oganessian and V. K. Utyonkov, *Rep. Prog. Phys.* **78**, 036301 (2015).
 - [4] C. Xu, X. Zhang, Z. Z. Ren, *Nucl. Phys. A* **898**, 24 (2013).
 - [5] J. Meng, Y. Chen, et al., *Phys. Scr. T* **154**, 014010 (2013).
 - [6] J. Jesús Mendoza-Temis, G. Martínez-Pinedo, et al., arXiv:1409.6135
 - [7] M. R. Mumpower, R. Surman, G. C. McLaughlin, A. Aprahamian, arXiv:1508.07352
 - [8] M. Liu, N. Wang, Z. X. Li, and F. S. Zhang, *Phys. Rev. C* **82**, 064306 (2010).
 - [9] N. Wang, M. Liu, H. Jiang, J. L. Tian, Y. M. Zhao, *Phys. Rev. C* **91**, 044308 (2015).

- [10] P. W. Zhao, Z. P. Li, J. M. Yao, and J. Meng, *Phys. Rev. C* **82**, 054319 (2010).
- [11] A. Sobiczewski, F.A. Gareev, B.N. Kalinkin, *Phys. Lett.* **22**, 500 (1966).
- [12] S. Hofmann and G. Münzenberg, *Rev. Mod. Phys.* **72**, 733 (2000).
- [13] N. Zeldes, *Phys. Lett. B* **429**, 20 (1998).
- [14] J.J. Li, W. H. Long, J. Margueron, N. V. Giai, *Phys. Lett. B* **732**, 169 (2014).
- [15] G.G. Adamian , N.V. Antonenko, and W. Scheid, *Eur. Phys. J. A* **41**, 235 (2009).
- [16] S. M. Lenzi and M. A. Bentley, *Lecture Notes in Physics*, **764**, 57 (2009).
- [17] S. Shlomo, *Rep. Prog. Phys.* **41**, 957 (1978)
- [18] N. Wang, M. Liu and X. Z. Wu, *Phys. Rev. C* **81**, 044322 (2010).
- [19] N. Wang, Z. Y. Liang, M. Liu and X. Z. Wu, *Phys. Rev. C* **82**, 044304 (2010).
- [20] M. Liu, N. Wang, Y. G. Deng, and X. Z. Wu, *Phys. Rev. C* **84**, 014333 (2011).
- [21] N. Wang, M. Liu, X. Z. Wu, and J. Meng, *Phys. Lett. B* **734**, 215 (2014).
- [22] N. Wang and M. Liu, *Phys. Rev. C* **84**, 051303(R) (2011); <http://www.imqmd.com/mass/>
- [23] Z. M. Niu, Z. L. Zhu, Y. F. Niu, et al., *Phys. Rev. C* **88**, 024325 (2013).
- [24] A. Sobiczewski, Yu. A. Litvinov, *Phys. Scr.* **T154**, 014001 (2013); *Phys. Rev. C* **89**, 024311 (2014).
- [25] Yu. A. Litvinov, M. Palczewski, E. A. Cherepanov, A. Sobiczewski, *Acta Phys. Polo. B* **45**, 1979 (2014).
- [26] Yu. Ts. Oganessian, V. K. Utyonkov, *Nucl. Phys. A* (2015), in press.
- [27] S. Cwoik, J. Dudek, W. Nazarewicz, J. Skalski, and T. Werner, *Comp. Phys. Comm.* **46**, 379 (1987).
- [28] F. Wienholtz, D. Beck, K. Blaum, et al., *Nature* **498**, 346 (2013).
- [29] N. Wang and M. Liu, *Chin. Sci. Bull.* **60**, 1145 (2015).
- [30] R. Orlandi, D. Mücher, R. Raabe, et al., *Phys. Lett. B* **740**, 298 (2015).
- [31] W. D. Myers, W. J. Swiatecki, *Nucl. Phys.* **81**, 1 (1966).
- [32] R. Janssens, *Nature* **435**, 897 (2005).
- [33] I. Angeli and K. P. Marinova, *J. Phys. G: Nucl. Part. Phys.* **42**, 055108 (2015).
- [34] K. Rutz, M. Bender, T. Bürvenich, T. Schilling, P.-G. Reinhard, J. A. Maruhn, and W. Greiner, *Phys. Rev. C* **56**, 238 (1997).
- [35] Q. Mo, M. Liu, N. Wang, *Phys. Rev. C* **90**, 024320 (2014).
- [36] Yu. Ts. Oganessian, V. K. Utyonkov, Yu. V. Lobanov, et al., *Phys. Rev. C* **74**, 044602 (2006).

- [37] I. Muntian, Z. Patyk, and A. Sobiczewski, *Phys. Atom. Nucl.* **66**, 1015 (2003).
- [38] I. Muntian, S. Hofmann, Z. Patyk, and A. Sobiczewski, *Acta Phys. Pol. B* **34**, 2073 (2003).
- [39] A. N. Kuzmina, G. G. Adamian, N. V. Antonenko, and W. Scheid, *Phys. Rev. C* **85**, 014319 (2012).
- [40] P. Möller, J. R. Nix, et al., *At. Data and Nucl. Data Tables* **59** (1995) 185.
- [41] Yu. Ts. Oganessian, V. K. Utyonkov, Yu. V. Lobanov, et al, *Phys. Rev. C* **70**, 064609 (2004).
- [42] V. K. Utyonkov, N. T. Brewer, Yu. Ts. Oganessian, et al, *Phys. Rev. C* **92**, 034609 (2015).